Quantum Fluctuations in Cosmology

Rafeh Rehan

April 2024

1 Introduction

Quantum fluctuations are a necessary consequence of the uncertainty principle. In non-relativistic (NR) quantum mechanics, it is the position and momentum of a particle that fluctuates. Analogously, in the relativistic formulation of quantum field theory (QFT), it is the field and it's canonical momentum that fluctuate. In early universe cosmology, NR quantum mechanics becomes insufficient at describing phases of highly energetic matter. Instead, QFTs are used to describe matter and their interactions with each other during this early epoch.

At approximately 10^{-43} seconds after the Big Bang, the Standard Model of Cosmology predicts a period where spacetime undergoes rapid expansion. During this Inflationary period, small scale physics plays a crucial role as tiny effects rapidly grow within fractions of a second. In particular, it is believed that vacuum fluctuations of quantum fields (and the metric) during inflation are the key ingredients needed to explain the large scale structure of our universe observed in matter distributions and the CMB [1].

In the following project, we attempt to illustrate how vacuum fluctuations of the Klein-Gordon (KG) field can give rise to a period of inflation in the early universe. In Section 2, we describe the mathematical and computational methods used to study quantum fluctuations of the spin 0 field described by solutions to the KG equation. Section 3 plots the results of numerical simulations for the KG field's fluctuations. Section 4 discusses the physical implications of our results, and applies them to the context of early universe cosmology. Section 5 proposes limitations on our approach, and identifies further directions for interesting study.

2 Methods

2.1 Solving the Spin-0 QFT in N+1 Minkowski Spacetime

We begin with the Klein-Gordon equation of motion in $N + 1$ dimensions

$$\left(\partial_t^2 - \Delta + m^2\right) \phi(\mathbf{x}, t) = 0 \tag{2.1}$$

with Dirichlet Boundary Conditions

$$\phi(\mathbf{x}_{boundary} = 0)$$

These boundary conditions enable us to solve this PDE with a Discrete Sine Fourier Transform (DSFT) after enforcing an infrared cutoff[1]. This Fourier transform is described by basis functions and orthogonality relations

$$b_n(x) := \sqrt{\frac{2}{L}} \sin\left(\frac{n\pi}{L}x\right)$$

$$\int_0^L b_n(x)b_m(x)dx = \delta_{nm} \tag{2.2}$$

with $n, m \in \mathbb{Z}$.

We find the DSFT and its inverse transform respectively using (2.2) for our field $\phi(\mathbf{x}, t)$. After IR regularization [2] in an N dimensional box $\Omega := [0, L]^N$, we obtain

$$\phi(\mathbf{x}, t) = \left(\frac{2}{L}\right)^{N/2} \sum_{n=1}^{\infty} \phi_{\mathbf{n}}(t) \prod_{i=1}^{N} \sin\left(\frac{n_i\pi}{L}x_i\right) \tag{2.3}$$

$$\phi_n(t) = \left(\frac{2}{L}\right)^{N/2} \int_{\Omega} \phi(\mathbf{x}, t) \prod_{i=1}^{N} \sin\left(\frac{n_i\pi}{L}x_i\right) d\mathbf{x} \tag{2.4}$$

where the sum in (2.3) occurs N times, iterating over each component $n_i \in \mathbb{Z}$, and $d\mathbf{x} = \prod_{i=1}^{N} dx_i$. Using this discrete Fourier mode decomposition for our original field $\phi(\mathbf{x}, t)$, it suffices to show

$$\Delta\phi(\mathbf{x}, t) = \left(\frac{2}{L}\right)^{N/2} \sum_{\mathbf{n}=1}^{\infty} \phi_{\mathbf{n}}(t) \left[\Delta \prod_{i=1}^{N} \sin\left(\frac{n_i\pi}{L}x_i\right)\right]$$

$$= \left(\frac{2}{L}\right)^{N/2} \sum_{\mathbf{n}=1}^{\infty} \phi_{\mathbf{n}}(t) \left[-\frac{n^2\pi^2}{L^2}\right] \prod_{i=1}^{N} \sin\left(\frac{n_i\pi}{L}x_i\right)$$

in order to show that each mode in our Fourier transformed field $\phi_{\mathbf{n}}(t)$ individually obeys the equation of motion

$$\left(\partial_t^2 + \omega_n^2\right)\phi_{\mathbf{n}}(t) = 0$$

$$\omega_n^2 := \frac{n^2\pi^2}{L^2} + m^2 \tag{2.5}$$

derived from (2.1) with the insertion of (2.3).

---

[1]This is done as we are concerned with the behaviour of our field within a finite measurement zone which can be described by a box $\Omega := [0, L]^N$, hence allowing us to exclude arbitrarily large spatially varying wave solutions

We now promote our discussion to that of a QFT by taking $\phi(\mathbf{x}, t) \to \hat{\phi}(\mathbf{x}, t)$, $\phi_{\mathbf{n}}(t) \to \hat{\phi}_{\mathbf{n}}(t)$ and enforcing Hermiticity and the Canonical Commutation Relations[2]

$$\hat{\phi}^{\dagger}(\mathbf{x}, t) = \hat{\phi}(\mathbf{x}, t) \tag{2.6}$$

$$\left[\hat{\phi}(\mathbf{x}, t), \dot{\hat{\phi}}(\mathbf{x}', t)\right] = i\delta^{(3)}\left(\mathbf{x} - \mathbf{x}'\right) \tag{2.7}$$

It is easier now to move to n-space in order to solve the differential equation (2.1), as we have shown that the Laplacian operator becomes multiplication by a factor dependent on n. The Hermiticity condition (2.6) straightforwardly implies in n-space, $\hat{\phi}^{\dagger}_{\mathbf{n}}(t) = \hat{\phi}_{\mathbf{n}}(t)$ directly from (2.4). The CCRs in (2.7) imply

$$\left[\hat{\phi}_{\mathbf{n}}(t), \dot{\hat{\phi}}_{\mathbf{n}'}(t)\right] = \left[\left(\frac{2}{L}\right)^{N/2} \int_{\Omega} \hat{\phi}(\mathbf{x}, t) \prod_{i=1}^{N} \sin\left(\frac{n_i \pi}{L} x_i\right) d\mathbf{x}, \left(\frac{2}{L}\right)^{N/2} \int_{\Omega} \dot{\hat{\phi}}(\mathbf{x}', t) \prod_{j=1}^{N} \sin\left(\frac{n_j' \pi}{L} x_j'\right) d\mathbf{x}'\right]$$

$$, = \left(\frac{2}{L}\right)^{N} \int_{\Omega} \int_{\Omega} \prod_{i=1}^{N} \sin\left(\frac{n_i \pi}{L} x_i\right) \prod_{j=1}^{N} \sin\left(\frac{n_j' \pi}{L} x_j'\right) \left[\hat{\phi}(\mathbf{x}, t), \dot{\hat{\phi}}(\mathbf{x}', t)\right] d\mathbf{x} d\mathbf{x}'$$

$$= i \left(\frac{2}{L}\right)^{N} \int_{\Omega} \prod_{i=1}^{N} \sin\left(\frac{n_i \pi}{L} x_i\right) \prod_{j=1}^{N} \sin\left(\frac{n_j' \pi}{L} x_j\right) d\mathbf{x}$$

$$= i\delta_{\mathbf{n}\mathbf{n}'}$$

where the last line follows from the orthogonality of (2.2). Hence, (2.6) and (2.7) together imply

$$\hat{\phi}^{\dagger}_{\mathbf{n}}(t) = \hat{\phi}_{\mathbf{n}}(t) \tag{2.8}$$

$$\left[\hat{\phi}_{\mathbf{n}}(t), \dot{\hat{\phi}}_{\mathbf{n}'}(t)\right] = i\delta_{\mathbf{n}\mathbf{n}'} \tag{2.9}$$

The equation of motion in (2.1) can be derived from the real space Hamiltonian operator [2]

$$\hat{H}(t) = \frac{1}{2} \int_{\mathbb{R}^N} \left(\dot{\hat{\phi}}^{\dagger}(\mathbf{x}, t)\dot{\hat{\phi}}(\mathbf{x}, t) + \hat{\phi}^{\dagger}(\mathbf{x}, t)\left(m^2 - \Delta\right)\hat{\phi}(\mathbf{x}, t)\right) d\mathbf{x} \tag{2.10}$$

In n space, after IR regularization, our Hamiltonian becomes

$$\hat{H}(t) = \sum_{\mathbf{n}} \left(\dot{\hat{\phi}}^{\dagger}_{\mathbf{n}}(t)\dot{\hat{\phi}}_{\mathbf{n}}(t) + \omega_n^2 \hat{\phi}^{\dagger}_{\mathbf{n}}(t)\hat{\phi}_{\mathbf{n}}(t)\right) \tag{2.11}$$

[2]Note, we work with natural units such that $\hbar = c = 1$

3

If we make the ansatz

$$\hat{\phi}_{\mathbf{n}}(t) = \frac{1}{\sqrt{2\omega_n}} \left(\hat{a}_{\mathbf{n}}^{\dagger}(t) + \hat{a}_{\mathbf{n}}(t) \right)$$

$$\dot{\hat{\phi}}_{\mathbf{n}}(t) = i\sqrt{\frac{\omega_n}{2}} \left(\hat{a}_{\mathbf{n}}^{\dagger}(t) - \hat{a}_{\mathbf{n}}(t) \right) \tag{2.12}$$

$$\hat{a}_{\mathbf{n}}(t) = \sqrt{\frac{\omega_n}{2}} \hat{\phi}_{\mathbf{n}}(t) + \frac{i}{\sqrt{2\omega_n}} \dot{\hat{\phi}}_{\mathbf{n}}(t)$$

with commutation relations for our new $\hat{a}_{\mathbf{n}}(t)$ operator[3]

$$\left[\hat{a}_{\mathbf{n}}(t), \hat{a}_{\mathbf{n}'}^{\dagger}(t) \right] = \left[\sqrt{\frac{\omega_n}{2}} \hat{\phi}_{\mathbf{n}}(t) + \frac{i}{\sqrt{2\omega_n}} \dot{\hat{\phi}}_{\mathbf{n}}(t), \sqrt{\frac{\omega_{n'}}{2}} \hat{\phi}_{\mathbf{n}'}(t) - \frac{i}{\sqrt{2\omega_{n'}}} \dot{\hat{\phi}}_{\mathbf{n}}(t) \right]$$

$$= -\frac{i}{2} \sqrt{\frac{\omega_n}{\omega_{n'}}} \left[\hat{\phi}_{\mathbf{n}}(t), \dot{\hat{\phi}}_{\mathbf{n}'}(t) \right] + \frac{i}{2} \sqrt{\frac{\omega_{n'}}{\omega_n}} \left[\dot{\hat{\phi}}_{\mathbf{n}'}(t), \hat{\phi}_{\mathbf{n}}(t) \right]$$

$$= \delta_{\mathbf{nn}'} \tag{2.13}$$

using (2.9). Then under our ansatz in (2.12), our Hamiltonian in n space given in (2.11) takes the form

$$\hat{H}(t) = \sum_{\mathbf{n}} \left(-\frac{\omega_n}{2} \left(\hat{a}_{\mathbf{n}}^{\dagger}(t) - \hat{a}_{\mathbf{n}}(t) \right)^2 + \omega_n^2 \cdot \frac{1}{2\omega_n} \left(\hat{a}_{\mathbf{n}}^{\dagger}(t) + \hat{a}_{\mathbf{n}}(t) \right)^2 \right)$$

$$= \sum_{\mathbf{n}} \omega_n \left(\hat{a}_{\mathbf{n}}^{\dagger}(t)\hat{a}_{\mathbf{n}}(t) + \hat{a}_{\mathbf{n}}(t)a_{\mathbf{n}}^{\dagger}(t) \right)$$

If we use our derived commutation relations for our ladder operators (2.13), our Hamiltonian simplifies to

$$\hat{H}(t) = \sum_{\mathbf{n}} \omega_n \left(\hat{a}_{\mathbf{n}}^{\dagger}(t)\hat{a}_{\mathbf{n}}(t) + \frac{1}{2} \right) \tag{2.14}$$

We can now simply derive the equations of motion for our new operator $\hat{a}_{\mathbf{n}}(t)$ via the Heisenberg equation

$$i\dot{\hat{a}}_{\mathbf{n}}(t) = \left[\hat{a}_{\mathbf{n}}(t), \hat{H}(t) \right]$$

$$= \sum_{\mathbf{n}} \omega_n \left[\hat{a}_{\mathbf{n}}(t), \hat{a}_{\mathbf{n}'}^{\dagger}(t)\hat{a}_{\mathbf{n}'}(t) \right] = \sum_{\mathbf{n}} \omega_n \left(\hat{a}_{\mathbf{n}}\hat{a}_{\mathbf{n}'}^{\dagger}\hat{a}_{\mathbf{n}'} - \hat{a}_{\mathbf{n}'}^{\dagger}\hat{a}_{\mathbf{n}'}\hat{a}_{\mathbf{n}} \right)$$

$$= \sum_{\mathbf{n}} \omega_n \left(\left(\delta_{\mathbf{nn}'} + \hat{a}_{\mathbf{n}'}^{\dagger}\hat{a}_{\mathbf{n}} \right) \hat{a}_{\mathbf{n}'} - \hat{a}_{\mathbf{n}'}^{\dagger}\hat{a}_{\mathbf{n}'}\hat{a}_{\mathbf{n}} \right) = \omega_n \hat{a}_{\mathbf{n}}$$

---

[3]Due to our Dirichlet boundary conditions, it is interesting to note that the states being created/annihilated here by our ladder operators are standing waves rather than propagating plane waves.

where the last equivalence is taken by using the fact that $\hat{a}_{\mathbf{n}}$ commutes with itself. This results in an equation of motion for each individual mode $\hat{a}_{\mathbf{n}}$

$$i\dot{\hat{a}}_{\mathbf{n}}(t) = \omega_n \hat{a}_{\mathbf{n}}(t) \tag{2.15}$$

which suggests a solution of the form

$$\hat{a}_{\mathbf{n}}(t) = \hat{a}_{\mathrm{in}_{\mathbf{n}}} e^{-i\omega_n t} \tag{2.16}$$

where $a_{\mathbf{n}}(t = 0) = \hat{a}_{\mathrm{in}_{\mathbf{n}}}$. We now have a mode decomposition for our scalar field in n space obtained from inserting our solution (2.16) into our ansatz (2.12)

$$\hat{\phi}_{\mathbf{n}}(t) = \frac{1}{\sqrt{2\omega_n}} \left(\hat{a}_{\mathrm{in}_{\mathbf{n}}}^{\dagger} e^{i\omega_n t} + \hat{a}_{\mathrm{in}_{\mathbf{n}}} e^{-i\omega_n t} \right) \tag{2.17}$$

We finish this section by justifying that the form of (2.17) solves our QFT. Note that the boundary conditions on $\hat{\phi}(\mathbf{x}, t)$ remain satisfied due to (2.3). It is Hermitian upon inspection and it also solves (2.5) since

$$\partial_t^2 \hat{\phi}_{\mathbf{n}}(t) = -\frac{\omega_n^2}{\sqrt{2\omega_n}} \left(\hat{a}_{\mathrm{in}_{\mathbf{n}}}^{\dagger} e^{i\omega_n t} + \hat{a}_{\mathrm{in}_{\mathbf{n}}} e^{-i\omega_n t} \right) = -\omega_n^2 \hat{\phi}_{\mathbf{n}}(t)$$

The CCRs in (2.9) are also satisfied due to (2.13)

$$\left[\hat{\phi}_{\mathbf{n}}, \dot{\hat{\phi}}_{\mathbf{n}'} \right] = \left[\frac{1}{\sqrt{2\omega_n}} \left(\hat{a}_{\mathbf{n}}^{\dagger} e^{i\omega_n t} + \hat{a}_{\mathbf{n}} e^{-i\omega_n t} \right), \frac{i\omega_{n'}}{\sqrt{2\omega_{n'}}} \left(\hat{a}_{\mathbf{n}'}^{\dagger} e^{i\omega_{n'} t} - \hat{a}_{\mathbf{n}'} e^{-i\omega_{n'} t} \right) \right]$$

$$= \frac{i\omega_{n'}}{2\sqrt{\omega_n \omega_{n'}}} \left\{ -\left[\hat{a}_{\mathbf{n}}^{\dagger}, \hat{a}_{\mathbf{n}'} \right] e^{i(\omega_n - \omega_{n'})t} + \left[\hat{a}_{\mathbf{n}}, \hat{a}_{\mathbf{n}'}^{\dagger} \right] e^{-i(\omega_n - \omega_{n'})t} \right\}$$

$$= \frac{i\omega_{n'}}{2\sqrt{\omega_n \omega_{n'}}} \left\{ \delta_{\mathbf{nn}'} e^{i(\omega_n - \omega_{n'})t} + \delta_{\mathbf{nn}'} e^{-i(\omega_n - \omega_{n'})t} \right\}$$

$$= i\delta_{\mathbf{nn}'}$$

2.2 Probability Amplitudes in the Schrodinger Picture

In order to simulate vacuum state quantum field fluctuations, we proceed by moving to the Schrodinger picture, in analogy to NR quantum mechanics. We define a *wave functional* $\Psi[\varphi(\mathbf{x}, t), t]$ in analogy to the NR wave function. Further, we define $|\Psi\rangle$ to be an eigenstate of our field operator with eigenfunctions $\varphi(t)$, $\tilde{\varphi}(t)$ such that

$$\hat{\phi}(\mathbf{x}, t) |\Psi\rangle = \varphi(\mathbf{x}, t) |\Psi\rangle \tag{2.18}$$

$$\hat{\phi}_{\mathbf{n}}(t) |\Psi\rangle = \tilde{\varphi}_{\mathbf{n}}(t) |\Psi\rangle \tag{2.19}$$

in real and n space Hilbert bases respectively. We further define the "field" representations of our state Ψ with

$$\Psi[\varphi, t] := \langle \varphi | \Psi \rangle$$

$$\Psi[\tilde{\varphi}, t] := \langle \tilde{\varphi} | \Psi \rangle$$

then we can represent the canonical commutation relations (2.7) through

$$\hat{\phi}(\mathbf{x}, t)\Psi[\varphi, t] = \varphi(\mathbf{x}, t)\Psi[\varphi, t]$$

$$\dot{\hat{\phi}}(\mathbf{x}, t)\Psi[\varphi, t] = -i\frac{\delta}{\delta\varphi(\mathbf{x}, t)}\Psi[\varphi, t] \tag{2.20}$$

The justification for this claim is obtained by computing

$$\left[\hat{\phi}(\mathbf{x}, t), \dot{\hat{\phi}}(\mathbf{x}', t)\right]\Psi[\varphi, t] = \hat{\phi}(\mathbf{x}, t)\dot{\hat{\phi}}(\mathbf{x}', t)\Psi[\varphi, t] - \dot{\hat{\phi}}(\mathbf{x}', t)\hat{\phi}(\mathbf{x}, t)\Psi[\varphi, t]$$

$$= \hat{\phi}(\mathbf{x}, t)\left(-i\frac{\delta}{\delta\varphi(\mathbf{x}', t)}\right)\Psi[\varphi, t] - \left(-i\frac{\delta}{\delta\varphi(\mathbf{x}', t)}\right)\varphi(\mathbf{x}, t)\Psi[\varphi, t]$$

$$= \hat{\phi}(\mathbf{x}, t)\left(-i\frac{\delta\Psi[\varphi, t]}{\delta\varphi(\mathbf{x}', t)}\right) + i\delta(\mathbf{x} - \mathbf{x}')\Psi[\varphi, t] + \varphi(\mathbf{x}, t)\left(i\frac{\delta\Psi[\varphi, t]}{\delta\varphi(\mathbf{x}', t)}\right)$$

$$= i\delta(\mathbf{x} - \mathbf{x}')\Psi[\varphi, t] + \left(\hat{\phi}(\mathbf{x}, t) - \varphi(\mathbf{x}, t)\right)\dot{\hat{\phi}}(\mathbf{x}, t)\Psi[\varphi, t]$$

$$= i\delta(\mathbf{x} - \mathbf{x}')\Psi[\varphi, t]$$

where the last line follows by removing the effect of the test functional and using (2.18). In n-space, an equivalent calculation can be done to represent the CCRs in (2.9). This translate to a representation given by

$$\hat{\phi}_{\mathbf{n}}(t)\Psi[\tilde{\varphi}, t] = \tilde{\varphi}_{\mathbf{n}}(t)\Psi[\tilde{\varphi}, t]$$

$$\dot{\hat{\phi}}_{\mathbf{n}}\Psi[\tilde{\varphi}, t] = -i\frac{\delta}{\delta\tilde{\varphi}_{\mathbf{n}}(t)}\Psi[\tilde{\varphi}, t] \tag{2.21}$$

In order to study vacuum state fluctuations of our quantum field, we solved the KG equation in 2.1. We proceed to identify the vacuum state of interest in the Schrodinger picture as $|\Psi\rangle = |0\rangle$ being that state in which for our chosen Fock basis used in (2.17), we expand the above as

$$\hat{a}_{\mathbf{n}}|\Psi\rangle = \hat{a}_{\mathbf{n}}|0\rangle = 0 \tag{2.22}$$

Let us define $\Psi_0[\tilde{\varphi}, t] := \langle \tilde{\varphi} | 0 \rangle$ as the ground-state wave functional of our system that is identified by the vacuum state of our QFT. Recalling our definitions for $\hat{a}_{\mathbf{n}}$ given in (2.12), we write in the "field" representation with the help of (2.21)

$$\hat{a}_{\mathbf{n}}\langle\tilde{\varphi}|\Psi\rangle = \left(\sqrt{\frac{\omega_n}{2}}\hat{\phi}_{\mathbf{n}}(t) + \frac{i}{\sqrt{2\omega_n}}\dot{\hat{\phi}}_{\mathbf{n}}(t)\right)\Psi_0[\tilde{\varphi}, t]$$

$$= \left(\sqrt{\frac{\omega_n}{2}}\tilde{\varphi}_{\mathbf{n}}(t) + \frac{1}{\sqrt{2\omega_n}}\frac{\delta}{\delta\tilde{\varphi}_{\mathbf{n}}(t)}\right)\Psi_0[\tilde{\varphi}, t] = 0$$

The last line defines a functional differential equation, and can be solved analogously to the quantum harmonic oscillator in 1st quantization [3]. We proceed by multiplying both sides by $\sqrt{2\omega_n}$

$$0 = \omega_n \tilde{\varphi}_{\mathbf{n}}(t) \Psi_0[\tilde{\varphi}, t] + \frac{\delta}{\delta \tilde{\varphi}_{\mathbf{n}}(t)} \Psi_0[\tilde{\varphi}, t]$$

$$-\omega_n \tilde{\varphi}_{\mathbf{n}}(t) = \frac{1}{\Psi_0[\tilde{\varphi}, t]} \frac{\delta \Psi_0[\tilde{\varphi}, t]}{\delta \tilde{\varphi}_{\mathbf{n}}(t)}$$

$$-\omega_n \tilde{\varphi}_{\mathbf{n}}(t) = \frac{\delta \log(\Psi_0[\tilde{\varphi}, t])}{\delta \tilde{\varphi}(t)}$$

$$\Rightarrow -\frac{\omega_n \tilde{\varphi}_{\mathbf{n}}^2(t)}{2} + C = \log(\Phi_0[\tilde{\varphi}, t])$$

exponentiating both sides, we find the vacuum state wave functional to be

$$\Psi_0[\tilde{\varphi}, t] = N e^{-\omega_n \tilde{\varphi}_n^2(t)/2} \tag{2.23}$$

up to normalization. After normalizing by using $\int_{-\infty}^{+\infty} e^{-\tilde{\varphi}_n^2} d\tilde{\varphi}_n = \sqrt{\pi}$, we obtain the ground state probability distribution,

$$|\langle \Psi_0 | \Psi_0 \rangle|^2 = \sqrt{\frac{\omega_n}{\pi}} e^{-\omega_n \tilde{\varphi}_n^2} \tag{2.24}$$

Just as in 1st quantization, $|\langle \psi(x) | \psi(x) \rangle|^2$ can be interpreted as the probability distribution that corresponds to finding the *position* of a particle at coordinate x,[4], $|\langle \Psi[\tilde{\varphi}_{\mathbf{n}}] | \Psi[\tilde{\varphi}_{\mathbf{n}}] \rangle|^2$ can be interpreted as the probability distribution that corresponds to finding the *field* in its $\mathbf{n}$-th mode.

2.3   Numerical Techniques

We take (2.24) to be the probability of finding the field amplitude in its $\mathbf{n}$-th mode. We use the inverse cumulative distribution method to draw samples from our obtained probability distribution in (2.24) [4]. The cumulative distribution function of (2.24) is

$$C(x) = \int_{-\infty}^{x} \sqrt{\frac{\omega_n}{\pi}} e^{-\omega_n \tilde{\varphi}_n^2} d\tilde{\varphi}_n = \frac{\mathrm{erf}(\sqrt{\omega_n} x) + 1}{2} \tag{2.25}$$

we can invert this denoting $y = C(x) \Rightarrow C^{-1}(y) = x$ and finding

$$C^{-1}(y) = \frac{\mathrm{erf}^{-1}(2y - 1)}{\sqrt{\omega_n}} \tag{2.26}$$

---

[4]Or rather, the probability of finding the particle in the interval $[x, x + dx]$

Equation (2.26) describes a map between a random number in the interval $[0,1]$ to a number that obeys the statistics of (2.24). This allows us a method to draw random samples obeying our distribution, allowing us to simulate quantum fluctuations of the KG field. Figure 2.1 shows an example of drawing values of $\tilde{\varphi}_{\mathbf{n}}$ via our inverse cumulative distribution function method.
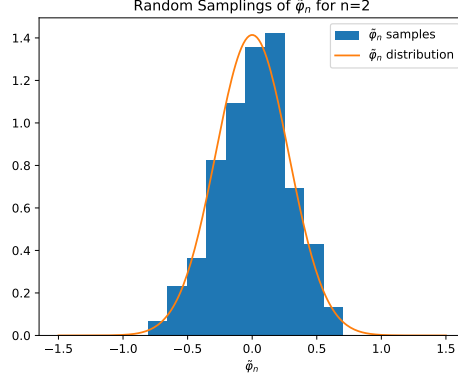

Figure 2.1: Probability distribution (2.24) for $n = 2$ (orange) and repeated samplings drawn from (2.26) (blue). 200 samples were taken by inputting a pseudo-random number between $[0,1]$ into (2.26) and normalizing the results.

A measurement of our quantum field $\hat{\phi}(\mathbf{x}, t)$ in theory yields a field amplitude, measured at all spaces and times, given by $\varphi(\mathbf{x}, t)$, which is fluctuating according to our probability distribution (2.24). Returning to (2.18), we can write using a truncated version of our DSFT given in (2.3)

$$\hat{\phi}(\mathbf{x}, t) \left| \Psi \right\rangle = \left[\left(\frac{2}{L} \right)^{N/2} \sum_{n=1}^{s} \hat{\phi}_{\mathbf{n}}(t) \prod_{i=1}^{N} \sin\left(\frac{n_i \pi}{L} x_i \right) \right] \left| \Psi \right\rangle$$

$$\varphi(\mathbf{x}, t) \left| \Psi \right\rangle = \left[\left(\frac{2}{L} \right)^{N/2} \sum_{n=1}^{s} \tilde{\varphi}_{\mathbf{n}}(t) \prod_{i=1}^{N} \sin\left(\frac{n_i \pi}{L} x_i \right) \right] \left| \Psi \right\rangle \qquad (2.27)$$

with s finite. With the truncated sum in (2.27), we can calculate and plot fluctuations in our field amplitude measurements $\varphi(\mathbf{x}, t)$ by obtaining Fourier coefficients $\varphi_{\mathbf{n}}(t)$ from our probability distribution (2.24) using the inverse cumulative distribution function (2.26) for each $n \leq s$. Physically, this results in an ultraviolet cutoff where we do not consider modes of higher frequency than s.

3 Results

Measurements of field amplitudes in (2.27) are evaluated using the methods proposed in 2.3. Simulations are executed using Python 3.11. Full code including packages used are available here.[5] To compute the inverse cumulative distribution function in (2.26), we use scipy's implementation of the error function and

---

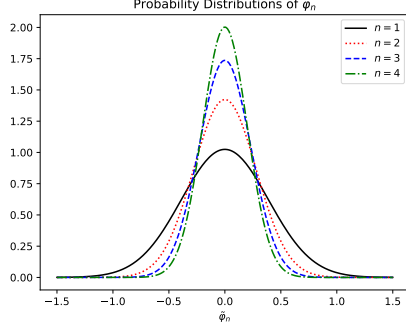[5]https://github.com/rafeh-rehan/qft-cosmo/blob/main/main.py

Figure 3.1: Probability distributions drawn from (2.24) for fixed $L = m = 1$ and varying n.
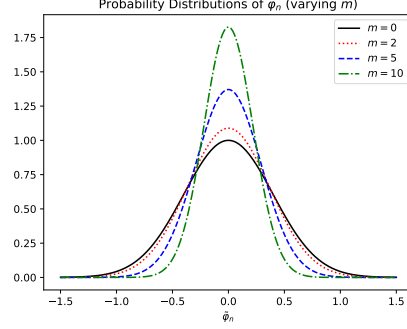
Figure 3.2: Probability distributions drawn from (2.24) for fixed $L = n = 1$ and varying m.

its inverse. We generate pseudorandom numbers for insertion into (2.26) using numpy. All plots are generated using matplotlib.

Probability distributions of the Fourier coefficient $\phi_{\mathbf{n}}$ drawn from (2.24) are shown in Figures 3.1, 3.2, 3.3. Figure 3.1 plots distributions of $\tilde{\varphi}_{\mathbf{n}}$ for various excited modes labelled by n. Figures 3.2 & 3.3 fix n, and plot the effect of varying m and L respectively. We use units in which $\hbar = c = 1$, as we are primarily interested in qualitative explanations of the quantum field's behaviour.
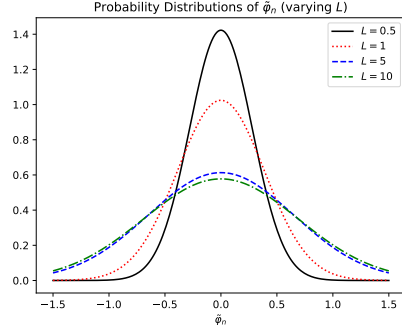

Figure 3.3: Probability distributions drawn from (2.24) for fixed $n = m = 1$ and varying L.

Field amplitudes calculated using (2.27) at constant time slices are shown for $N = 2, 3$ spatial dimensions in Figures 3.4 & 3.5 respectively[6]. To observe the effect of the box $\Omega = [0, L]^N$ and mass of the field m, Figures 3.6 & 3.7 plot field amplitudes while holding all parameters fixed except L and m respectively for $N = 3$.

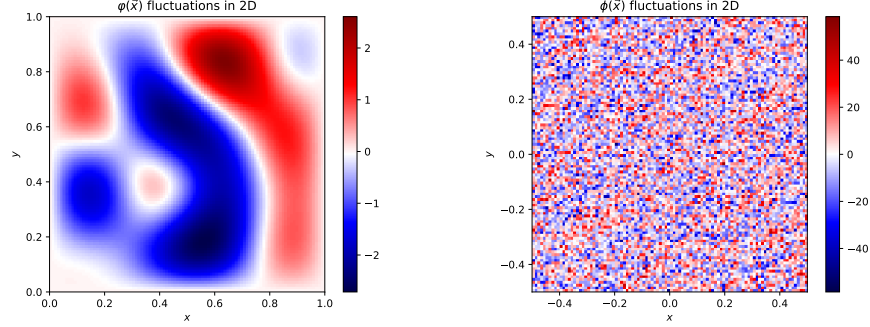[6]For $N = 3$, we set $z = 1/2$ for comparison with the $N = 2$ case.

Figure 3.4: Contour plots of field amplitude measurements $\varphi(\mathbf{x})$ for $N = 2$. The sum was computed for $s = 4$ (left) and $s = 400$ (right) terms.
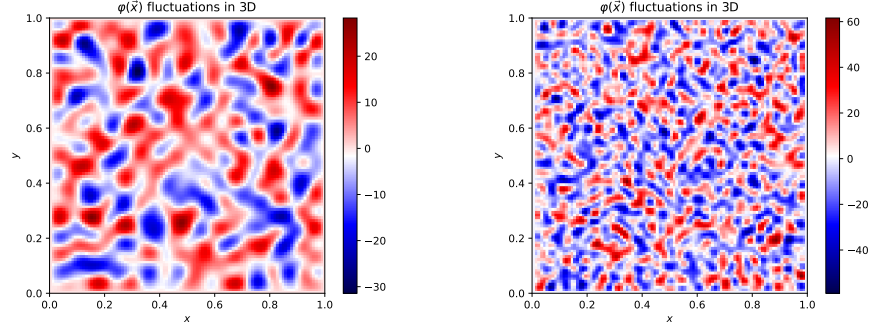

Figure 3.5: Contour plots of field amplitude measurements $\varphi(\mathbf{x})$ for $N = 3$ spatial dimensions. The sum was performed for $s = 20$ (left) and $s = 40$ (right) terms.

4 Discussion

4.1 Physics of Spin-0 Quantum Field Fluctuations

We begin this section with explanations of the simulated physics presented in Section 3. In particular, we discuss the role of our choice of truncation parameter s, mass, volume, and spatial dimensions N on vacuum fluctuations of the KG field's amplitude. As an initial check, we examine Figure 3.1 to check limiting n cases of vacuum field fluctuations. We notice that the distributions become sharper around 0 for increasing frequencies labelled by n. This is expected since higher frequency modes have higher energy and thus, are less energetically favourable to be created by vacuum fluctuations. This behaviour is opposed to that of the lower frequency modes (small n), which are energetically favoured in the vacuum state. We obtain then the expected result, that the primary contri-
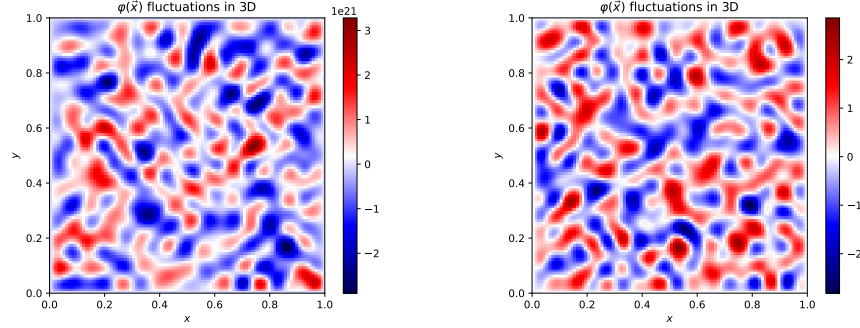
Figure 3.6: Contour plots of $\varphi(\mathbf{x})$ in $N = 3$. The sum was computed for fixed $s = 20$, $m = 1$ while varying the size of the 3 dimensional box to side lengths $L = 10^{-20}$ (left) and $L = 10$ (right).
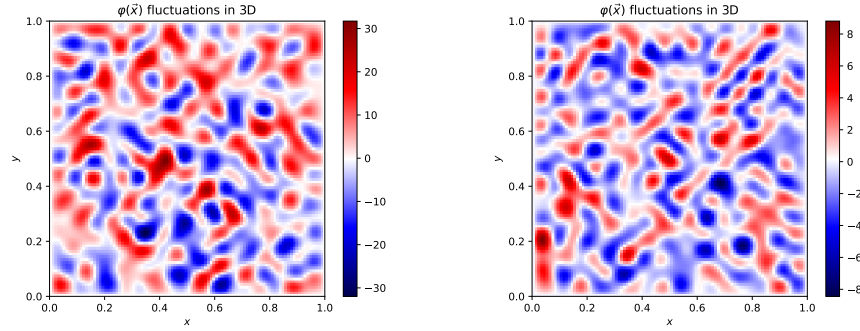

Figure 3.7: Contour plots of $\varphi(\mathbf{x})$ in $N = 3$. The sum was computed for fixed $s = 20$, $L = 1$ while varying the mass of the KG field quanta with $m = 0$ (left) and $m = 10^3$ (right).

bution to the amplitude's fluctuations in the vacuum state come from smaller frequency (low energy) normal modes.

Further, we argue that the choice of truncation parameter s is the same as a choice of Ultraviolet cutoff. This can be seen by considering the field amplitude's dependence on s illustrated in 2 spatial dimensions in Figure 3.4. Here, the choice of small s results in limited fluctuations of small magnitude, while large s produces larger amplitudes and more dense fluctuations. The choice of s in (2.27) corresponds to a decision about the maximum considered frequency of normal modes of the system. When we consider a maximum frequency that is relatively small, then we are considering only small energy fluctuations, even though in reality there is a non-zero probability for higher energy fluctuations. In the $s = 400$ case, we see that if we do consider these higher frequency modes, then the amplitude of our fluctuations increase and more complex wave pat-

terns emerge from the increase of interference between superposed modes. This suggests that in the "Ultraviolet" limit as $s \to \infty$, the sum in (2.27) diverges towards infinity and so our QFT necessitates an Ultraviolet cutoff synonymous with a choice of finite s.

The effect of the KG field's mass, and the volume of the box considered from the Infrared cutoff performed in Section 2 also play a visible role in the field's fluctuations. Figures 3.2 & 3.7 illustrate how increasing the field's mass reduces the probability of obtaining field amplitudes of large magnitude, and thus, large fluctuations. Alternatively, as we decrease the mass of the field towards zero, the distribution asymptotes towards a fixed shape.

In a non-relativistic situation, we would expect fluctuations to blow up as $m \to 0$ for harmonic oscillators[7] with frequency $\omega = \sqrt{K/m}$. However, in the relativistic scenario described by the KG equation, the frequency dependency is instead given in the form of (2.5), which does not blow up as $m \to 0$ and instead asymptotes towards a purely "momentum" driven frequency. Alternatively, this can be understood as more massive fields, which correspond to more massive field quanta/particles, require more energy to create from vacuum fluctuations, and are thus energetically suppressed.

Increasing the mass and increasing the mode n thus have the same effect on the probability distributions of modes $\tilde{\varphi}(\mathbf{x})$, for essentially the same reason. Higher energy quanta of the field require too much energy to be consistently produced via vacuum fluctuations of our QFT's ground state. In the case of decreasing/increasing the volume of the box however, the effect is reversed. The probability distributions of the $n = 1$ mode in the ground state in Figure 3.3 becomes peaked around 0 for *small* values of our parameter L this time, and asymptotes to a fixed, spread curve as L grows. The effect of this on the fluctuations of $\varphi(\mathbf{x})$ can be observed by comparing the $s = 20$ case in Figure 3.5 to Figure 3.6. We find that the fluctuations of $\varphi(\mathbf{x})$ become more intense.

This means that the chances of creation (and annihilation) of normal modes n remains fixed as the volume of our box (established during IR regularization) grows. However, the fluctuations in the field decrease by virtue of the uncertainty principle. As the uncertainty of the field amplitude (analogous to the position variable) increases with an increasing box size, the uncertainty in the field's momentum amplitude (analogous to the momentum variable) reduces, and approaches the field's momentum in the vacuum, which in inertial Minkowski space, is the no particle state.[8]

In the plots of the field amplitude $\varphi(\mathbf{x})$, we also notice that the $N = 3$

---

[7]Both classical and quantum.

[8]Note that the field amplitude does not reduce to zero if we increase the maximum mode considered in the truncated sum (2.27). However, a cutoff must be taken regardless to avoid an ultraviolet divergence. I imagine this is why renormalization is important since the dependence of the field on parameters such as L can in general depend on the choice of this cutoff, which is an upper limit choice on the frequency/energy of field quanta (a UV cutoff).

case has much larger amplitudes on average. As there is an additional spatial dimension, quantum fluctuations both above and below the hyperplane $z = 1/2$ contribute to the fluctuations on the surface of the plane, amplifying the strength of the fluctuations compared to the case of two spatial dimensions.

4.2 Cosmological Implications

In classical GR, the potential of a scalar field manifests in the Einstein equations. In particular, if we assert that the KG field is the largest contributing factor to the energy-momentum tensor, then for the μ, $\nu = 0$ term in the the Einstein equations, we have

$$3\left(\frac{\dot{a}}{a}\right)^2 = 8\pi G T^0{}_0 + \Lambda \tag{4.1}$$

where $a(t)$ is the scale factor associated with universal expansion, $T^0{}_0$ is the energy density of our KG field given by

$$T^0{}_0 := \rho(t) = \frac{1}{2}\dot{\phi}^2 + V(\phi) \tag{4.2}$$

and Λ is the cosmological constant producing the expansion of our universe [1]. Putting the two equations together,

$$3\left(\frac{\dot{a}}{a}\right)^2 = 8\pi G \left(\frac{1}{2}\dot{\phi}^2 + V(\phi)\right) + \Lambda \tag{4.3}$$

Hence, if there exists a time in our universe that satisfies the condition $V(\phi) \gg \dot{\phi}^2/2$, then (4.3) would reduce to

$$3\left(\frac{\dot{a}}{a}\right)^2 = 8\pi G V(\phi) + \Lambda$$

then the scalar potential $V(\phi)$ can play the exact same role as Λ does, namely, it can make spacetime expand. Hence, the potential of a scalar field $V(\phi)$ can serve as a mechanism for a period of cosmological inflation as long as the condition $V(\phi) \gg \dot{\phi}^2/2$ is met in the early universe . The fluctuations of the field amplitude $\varphi(\mathbf{x})$ explored in Section 4 imply that if we were to observe a small region of space in the limit as L approaches the Planck length, we would have a good chance of obtaining large fluctuations, and thus, large values of the field amplitude $\varphi(\mathbf{x})$.[9] This would translate to a large value of $V(\phi)$[10], and thus a large "cosmological constant", which corresponds to a period of incredibly rapid expansion.

---

[9]The probability may be tiny, but in a large universe, we only need to require this to happen just once for inflation to take off.

[10]When the potential takes the form of a power law expansion of even powers usually.

Thus, an inflationary period is predicted to begin in a small region of space in the early universe. We now consider a finite time later after inflation has begun. Under the subsequent expansion of spacetime, the original box with side lengths of order l_{planck} will soon expand to galactic sizes. From our discussion of the effect of L on the fluctuations of the field, we know that for large L,[11] the contribution to the amplitude from higher modes will be suppressed and the overall averaged field amplitude of $\varphi(\mathbf{x})$ will be significantly smaller. Thus as a consequence of inflation, the resulting decrease in $\varphi(\mathbf{x})$ will reach a critical point where $V(\phi)$ reduces to the point where it no longer produces an accelerated expansion. Thus, the mechanism for the beginning of inflation also results in its end.

5   Conclusion

In a limited treatment, we have attempted to describe how a period of inflation could arise in the early universe through quantum fluctuations of the Klein-Gordon field on a classical Minkowski background metric. However, in our discussion we have excluded more realistic models of spacetime that describe an expanding universe. Crucial physics that is paramount to understanding the mechanism of inflation and the evolution of our universe has thus been ignored. Interesting effects such as particle creation through spacetime expansion, quantized linear metric fluctuations, and symmetry breaking of the inflaton field at the end of inflation, all play a key role in the subsequent structure formation of matter distribution and the CMB through inhomogeneities seeded during the beginning of inflation [1][2].

These directions could be pursued by extending our discussion here to a Friedmann–Lemaître–Robertson–Walker (FRLW) metric, which is conformally related to the Minkowskian metric under a suitable coordinate transformation. It would also be interesting to explore what vacuum fluctuations of the KG field look like for an accelerated observer using our simulation techniques. Because an accelerated observer never sees a 0 particle vacuum state due to the Unruh effect [2], excited modes should have higher field amplitude fluctuations than for a non-accelerating Minkowski observer. One could extend this discussion further to accelerated observers in an FRLW spacetime to explore how the Unruh effect manifests on a background spacetime that is also expanding.

References

1. Carroll, S. M. *Spacetime and Geometry: An Introduction to General Relativity* (Cambridge University Press, 2019).

2. Mukhanov, V. F. & Winitzki, S. *Introduction to Quantum Fields in Classical Backgrounds* Lecture Notes. 2004.

---

[11] And fixed s.

3. Griffiths, D. J. & Schroeter, D. F. *Introduction to Quantum Mechanics* 3rd ed. (Cambridge University Press, 2018).

4. Devroye, L. *Non-Uniform Random Variate Generation* (Springer-Verlag, New York, NY, USA, 1986).